

# Intermediates and Products of Ethanol Oxidation on Platinum in Acid Solution

B. Bittins-Cattaneo, S. Wilhelm, E. Cattaneo, H. W. Buschmann, and W. Vielstich

Institut für Physikalische Chemie, Universität Bonn, Wegelerstraße 12, 5300 Bonn 1, Federal Republic of Germany

*Adsorption / Catalysis / Electrooxidation / Mass Spectrometry / Spectroscopy, Infrared*

The adsorbate formed during ethanol oxidation in acidic solutions is studied by Fourier transform infrared reflection-absorption spectroscopy (FTIR) at constant potential, on-line (DEMS) and thermal desorption mass spectroscopy (ECTDMS). — As in the case of methanol adsorbate  $\text{CO}_{\text{ad}}$  was identified by FTIR and in addition  $\text{COH}_{\text{ad}}$  by ECTDMS. On-line MS experiments showed the formation of methane during the cathodic sweep of the voltammogram. Main products of ethanol oxidation from the bulk are carbon dioxide and acetaldehyde.

## Introduction

The electrooxidation of  $\text{C}_2\text{H}_5\text{OH}$  on platinum in acid electrolytes is of general importance for catalytic processes at metal electrodes. During chemisorption at a platinum surface a strongly adsorbed intermediate is formed which is oxidized above +450 mV versus RHE. The position of the oxidation peak in a cyclic voltammogram near 0.7 V is not characteristic for ethanol. The oxidation of the adsorbates of  $\text{CH}_3\text{OH}$ ,  $\text{HCOOH}$  and reduced  $\text{CO}_2$  occurs almost at the same potential [1]. This common nature of the strongly adsorbed species may be due to the fact that in all cases an oxygen atom is needed to form  $\text{CO}_2$ . The oxygen atom is only available via formation of chemisorbed oxygen at the electrode surface, which begins at a characteristic potential for platinum.

Up to the present two experimental techniques have been used to study the nature of the ethanol adsorbate. Willsau and Heitbaum [2] used an electrochemical mass spectroscopic technique in combination with labelled isotopes. In the presence of bulk ethanol  $\text{CO}_2$  and  $\text{CH}_3\text{CHO}$  were found as volatile products. This is in accordance with a mechanism proposed earlier [3]. During the oxidation of the ethanol adsorbate (after exchange of electrolyte) only  $\text{CO}_2$  was observed. Using  $\text{CH}_3\text{CH}_2^{18}\text{OH}$  for the adsorption step in 0.5 M  $\text{H}_2\text{SO}_4 + \text{H}_2^{18}\text{O}$  and  $\text{H}_2^{16}\text{O}$  during oxidation,  $\text{C}^{16}\text{O}^{16}\text{O}$  and  $\text{C}^{18}\text{O}^{16}\text{O}$  in a ratio of about 1 : 2.5 were found in MS analysis. From this observation the authors concluded:

- $\text{C}^{16}\text{O}^{16}\text{O}$  is formed via reaction of a short-lived  $\text{CH}_3$  radical with water,
- the adsorbed intermediate contains the intact C—C bond, and in consequence,
- the ethanol adsorbate is NOT  $\text{CO}_{\text{ad}}$  [4].

Beden et al. [5] made an in-situ analysis of the ethanol adsorbate by electrochemically modulated IRRAS, a technique called EMIRS. The electrochemical modulation was done with 13.6 Hz and 400 mV difference in potential. The signal to noise ratio was not improved any more when more than 50–60 spectra are accumulated. Typically one scan over  $400\text{ cm}^{-1}$  needs 4 min.

A very intense band was detected for Pt in 0.1 M  $\text{C}_2\text{H}_5\text{OH} + 0.5\text{ M HClO}_4$  solution around  $2070\text{ cm}^{-1}$  with a peak-to-peak amplitude up to  $10^{-3} \Delta R/R$ . This band corresponds

to linearly bonded CO, a band already observed for  $\text{CH}_3\text{OH}$ ,  $\text{HCOOH}$  and ethylene glycol. Other smaller signals were difficult to interpret.

In this paper we like to clarify the contradicting results in the literature by introducing a third technique, ECTDMS [6, 7]. In addition new experimental results using on-line mass spectroscopy as well as in-situ FTIR spectroscopy are reported.

## Experimental

### Chemicals

Electrolyte solutions were prepared with Millipore water and analytical grade chemicals:  $\text{H}_2\text{SO}_4$  (Merck),  $\text{CH}_3\text{CH}_2\text{OH}$  (Merck),  $\text{CH}_3\text{CHO}$  (Merck) and  $^{12}\text{CH}_3^{13}\text{CH}_2\text{OH}$  (99.6 atom %  $^{13}\text{C}$ , MSD Isotopes). As base electrolyte 0.05 M  $\text{H}_2\text{SO}_4$  was chosen to minimize anion adsorption.

All solutions were carefully deaerated with Ar (99.996%) and further purified through Oxsorb (Messer Griesheim).

### On-Line MS Technique

The experiments were performed in a flow cell made out of plexi glass containing approximately 2 ml of solution [8]. The working electrode was a Pt layer prepared from a Pt suspension (DODUCO, mean particle size  $5\text{ }\mu\text{m}$ ) applied on a PTFE membrane. The real surface area varied between 6 and  $11\text{ cm}^2$ . Potentials were measured versus a reversible hydrogen electrode in the same solution. A Pt wire served as counter electrode. For details see Ref. [8].

In order to avoid contamination with air the solution containers were connected to the cell by glass tubes only and the entire Ar flow system was made of steel capillaries.

For the on-line detection of volatile reaction products (DEMS) the electrochemical cell was connected to a quadrupole mass spectrometer\*) as described in details elsewhere [10].

The controlling of the quadrupole analyzer and the registration of the current/potential output of the potentiostat were achieved by a PC computer. As function of electrochemical potential or time up to 7 masses were recorded simultaneously, the time interval for setting each mass value being 250 ms.

### Transfer System and TDMS Device [11]

A detailed description of the principle of the ECTDMS method (Electrochemical Thermal Desorption Mass Spectroscopy) has already been given [6]. In the meantime, however, we have considerably improved the design of our TDMS device (see Fig. 1).

\*) In earlier experiments magnetic field mass spectrometers have been used for this type of electrochemical mass spectroscopy [9].

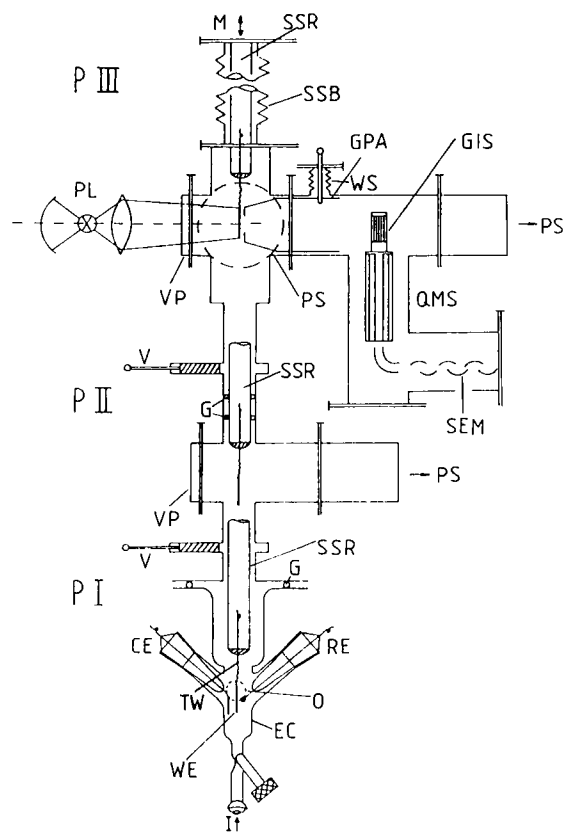


Fig. 1

## Experimental set up for ECTDMS.

P I: Electrode in the electrochemical cell, P II: Electrode in the lock chamber, P III: Electrode in UHV analysis position. CE: counter electrode; EC: electrochemical cell, GIS: grid ion source; GMS: glass-to-metal seal; GPA: gold-plated aperture; I: inlet for electrolyte, M: motor; O: outlet for electrolyte; PL: projector lamp with optical system; PS: pumping system; QMS: Quadrupole Mass Spectrometer with Secondary Electron Multiplier (SEM); RE: reference electrode; SSR: stainless steel rod; TW: thermocouple wires; V: valve; VP: viewport; WE: working electrode; WS: wobble stick

During a typical ECTDMS-experiment the electrode will pass three different positions.

## Position I:

The electrode is in the cell where the adsorption layer is formed electrochemically via a flow cell procedure.

## Position II:

The electrode is in the lock chamber. After the valve V has been closed the pumping system PS (consisting of a turbomolecular pump and a rotary pump) is switched on, and a pressure of  $10^{-6}$  torr is obtained in about 5 minutes.

## Position III:

The electrode is in the surface analysis position in the UHV chamber (base pressure about  $8 \cdot 10^{-9}$  torr). The upper valve V is closed, and the gold-plated copper aperture GPA is positioned tightly behind the electrode by means of a wobble stick WS (gap about 1 mm). The electrode is heated through the viewport VP by the thermal radiation of a 1000 W projector lamp PL, the heating coils are projected by a simple optical system onto one side of the electrode. The detected particles will mainly come from the other side of the electrode, which is not illuminated. Thus, there is a direct line of sight between the Pt sample analyzed and the grid ion source

GIS of the mass spectrometer. Collisions between the desorbed particles and the walls of the system are substantially reduced.

The Quadrupole Mass Spectrometer is supplied with a multiple ion detection system.

The UHV chamber is evacuated by two different pumping system PS, both consisting of a turbo molecular pump, a rotary pump and an oil diffusion pump as additional booster pump. The stainless steel rod is motor driven, and the stainless steel bellows allows a travel of 600 mm.

## Electrochemical Cell (ECTDMS)

The electrochemical cell (Fig. 2) has a volume of about 8 ml. The use of porous glass sinters to separate compartments for the reference and counter electrode is avoided in order to facilitate the complete exchange of solutions (flow cell procedure). For the same reason, the reference electrode, a platinized Pd net charged with hydrogen, was placed in the cell without a Luggin capillary.

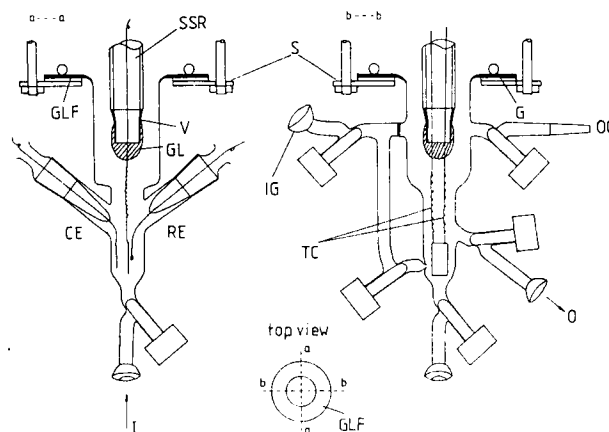


Fig. 2

## Electrochemical cell used for ECTDMS measurements.

CE: counter electrode; G: gasket; GL: glass; GLF: glass flange; I: inlet for electrolyte; IG: inlet for gas; O: outlet for electrolyte; OG: outlet for gas; RE: reference electrode; S: screwing; SSR: stainless steel rod; TC: Pt-Pt/Rh-thermocouple; V: Viton

The different electrolytic solutions are flowing into the cell compartment from below via glass tubes by slightly pressurizing the storage flasks. The cell has a glass flange on its top, and is screwed onto the apparatus via a viton-o-ring.

## Working Electrode (ECTDMS)

The working electrode used for the ECTDMS measurements consists of a smooth Pt sheet of  $10 \times 20 \times 0.1$  mm<sup>3</sup> with a roughness factor *R* of about 1.3. In order to get a clean Pt surface free of carbon the sample was heated in an oxygen atmosphere for a prolonged time (5–10 h) before the first experiment was performed ( $p_{O_2}$ , ca.  $2 \cdot 10^{-6}$  torr,  $T = 850$  K) [6]. A short period of heating in oxygen ( $p_{O_2}$ , ca.  $1 \cdot 10^{-6}$  torr,  $T = 850$  K, 10 minutes) was repeated at the beginning of each experiment.

## FTIR

In-situ IR spectroscopy, a relatively new thin layer technique, can identify submonolayers of dipoles formed on electrodes during adsorption, oxidation or reduction of active species [12, 13]. The main experimental problem in measuring spectra of an electrode-electrolyte interface is associated with absorption of most of the IR radiation by the solvent.

Due to surface selection rules only the light component with the electric field vector parallel to the plane of reflection, p-polarized light, can transfer energy to the dipoles adsorbed at the electrode surface. The sensitivity problem can be overcome by modulation of

either electrode potential (EMIRS, electrochemically modulated infrared spectroscopy) or light polarisation (PMIRRAS, polarisation modulated infra-red reflection-adsorption spectroscopy). We have used SNIFTIRS, a Fourier transform version of EMIRS (for details see [13] or [14]).

The infrared spectrometer used was a Digilab FS40 Fourier transform instrument, with a liquid nitrogen-cooled Mercury Cadmium Telluride, (MCT), detector. The instrument is provided with a computer for data acquisition, storage and mathematical treatment; p-polarised incident light was obtained by means of a BaF<sub>2</sub>-supported aluminium grid polariser # 312900, Oriel. CaF<sub>2</sub> was used as IR window.

The working electrodes, 15 mm diameter discs of polycrystalline platinum fixed in an araldite body, were mechanically polished with alumina or diamond paste down to 0.05 µm, dipped in diluted HNO<sub>3</sub> followed by rinsing with ultrasonic application.

The necessary thin-layer configuration was obtained by pressing the electrode against the optical window. A micrometer screw attached to the working electrode allows a reproducible adjustment of electrode-window distances.

## Results

### 1. Bulk Oxidation of Ethanol

Fig. 3 shows our results (a) current and (b) simultaneously recorded mass signals for volatile species formed during the oxidation of <sup>12</sup>CH<sub>3</sub><sup>13</sup>CH<sub>2</sub>OH in 0.05 M H<sub>2</sub>SO<sub>4</sub> solution. The peaks in current and mass intensity refer to each other. Beside a heavy CO<sub>2</sub> production (not shown in Fig. 3) potential dependent mass signals for *m/e* = 15 and 30 can be detected. Mass 15 represents the M1-signal of <sup>12</sup>CH<sub>4</sub> methane formed by the cleavage of one H-atom in the ionization source; mass 30 is the main fragment of <sup>12</sup>CH<sub>3</sub><sup>13</sup>CHO acetaldehyde. Simultaneously masses *m/e* = 29 (main fragment of <sup>12</sup>C<sup>13</sup>CH<sub>6</sub> ethane), *m/e* = 31 (main fragment of <sup>12</sup>CH<sub>3</sub>OH methanol) and *m/e* = 32 (main fragment of <sup>13</sup>CH<sub>3</sub>OH and <sup>12</sup>CH<sub>3</sub><sup>13</sup>CH<sub>2</sub>OH ethanol) were recorded. For these mass sig-

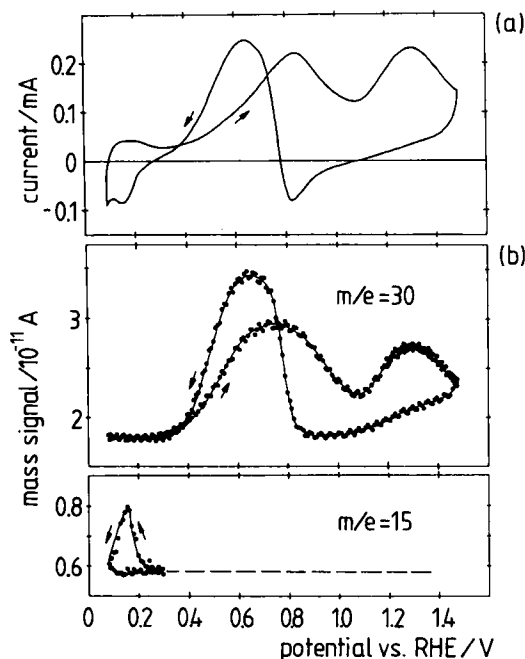


Fig. 3

Oxidation of bulk ethanol in a 0.05 M H<sub>2</sub>SO<sub>4</sub> + 0.01 M <sup>12</sup>CH<sub>3</sub><sup>13</sup>CH<sub>2</sub>OH solution; *v* = 10 mV/s (a) current (b) mass signal for *m/e* = 15 and 30

nals no potential dependence above the respective base intensity could be detected.

The possible contribution of a strongly bonded intermediate to the reaction products CO<sub>2</sub>, methane and acetaldehyde is studied by flow cell technique.

### 2. Study of the Adsorbate by Flow Cell Procedure

The flow cell procedure used here is described in detail elsewhere [8]. Ethanol and acetaldehyde adsorbates were formed out of 0.05 M H<sub>2</sub>SO<sub>4</sub> + 0.01 M <sup>12</sup>CH<sub>3</sub><sup>13</sup>CH<sub>2</sub>OH and 0.05 M H<sub>2</sub>SO<sub>4</sub> + 0.01 M CH<sub>3</sub>CHO solutions, respectively. Isotope labelled ethanol was used to distinguish between the oxidation products of the alcoholic and methyl group of ethanol. The adsorption potential *E*<sub>ad</sub> was varied between 150 mV and 600 mV and the adsorption time *t*<sub>ad</sub> between 20 s and 20 min. During adsorption current and mass signals were followed. The adsorption was interrupted by replacing the solution by pure supporting electrolyte under potential control. Afterwards a potential sweep was started in cathodic or anodic direction and the current/mass spectra for desorption of the adsorbate were recorded. The second sweep was taken as a proof that the electrolyte exchange was complete and no adsorbate remained on the electrode. The degree of coverage with adsorbate *θ*, depending on *E*<sub>ad</sub> and *t*<sub>ad</sub>, was evaluated from the suppression of hydrogen coverage.

A typical current/mass intensity-potential sweep of an ethanol adsorbate formed at *E*<sub>ad</sub> = 400 mV during *t*<sub>ad</sub> = 200 s starting in cathodic direction is shown in Fig. 4: (a)

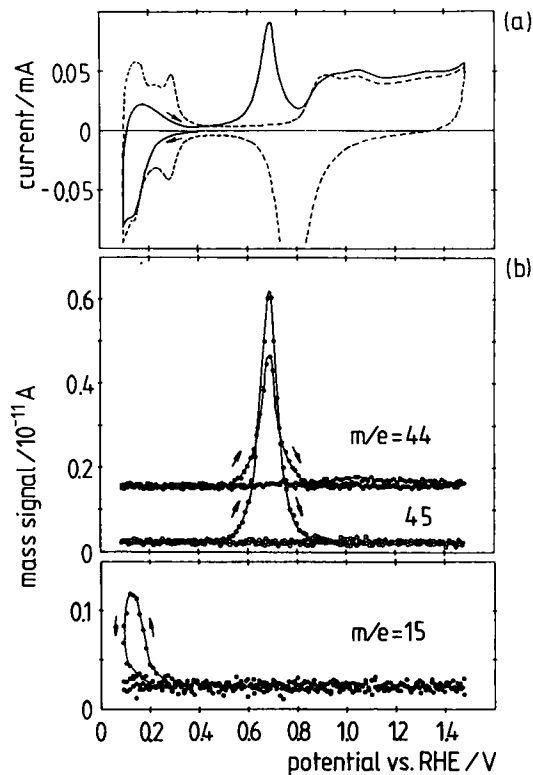


Fig. 4

Oxidation profile of ethanol adsorbate formed out of a 0.05 M H<sub>2</sub>SO<sub>4</sub> + 0.01 M <sup>12</sup>CH<sub>3</sub><sup>13</sup>CH<sub>2</sub>OH solution (*E*<sub>ad</sub> = 400 mV, *t*<sub>ad</sub> = 200 s, *θ* = 0.86); *v* = 10 mV/s; (a) current (---) base electrolyte and (b) mass signal for *m/e* = 15, 44 and 45

current and (b) mass signals for  $m/e = 15, 44$  and  $45$ . Two different kinds of  $\text{CO}_2$ , namely  $^{12}\text{CO}_2$  ( $m/e = 44$ ) and  $^{13}\text{CO}_2$  ( $m/e = 45$ ) are detected having the same peak potential. Mass 15 represents methane (see above). Simultaneously masses  $m/e = 29, 30, 31$  and  $32$  were recorded. For these masses no potential dependence above the respective base signal could be detected.

Similar experiments were performed for ethanol adsorbates formed at adsorption potentials  $E_{\text{ad}}$  between 150 and 600 mV, that is in the hydrogen adsorption region and (above 300 mV) in the region of acetaldehyde formation (see Fig. 3). Thus for constant adsorption times  $t_{\text{ad}} = 200$  s the coverage degree of adsorbate  $\theta$  was varied between 0.05 and 0.87. The maximum coverage is reached near 350 mV, variation of  $t_{\text{ad}}$  between 20 s and 20 min at this potential causes only minor changes in  $\theta$ .

As reaction products of all adsorbates only  $^{12}\text{CH}_4$ ,  $^{12}\text{CO}_2$  and  $^{13}\text{CO}_2$  (no acetaldehyde) could be detected, the relative amount of each species depending on  $E_{\text{ad}}$ .  $^{12}\text{CH}_4$  is only formed in the reductive scan at potentials lower than 250 mV (i.e. in the hydrogen region). During ethanol adsorption at potentials  $E_{\text{ad}} < 200$  mV methane is produced to a large extent. This is evident from the adsorption transient recorded for  $m/e = 15$ . In the subsequent reductive potentiodynamic scan no further methane signal above the base signal can be detected.

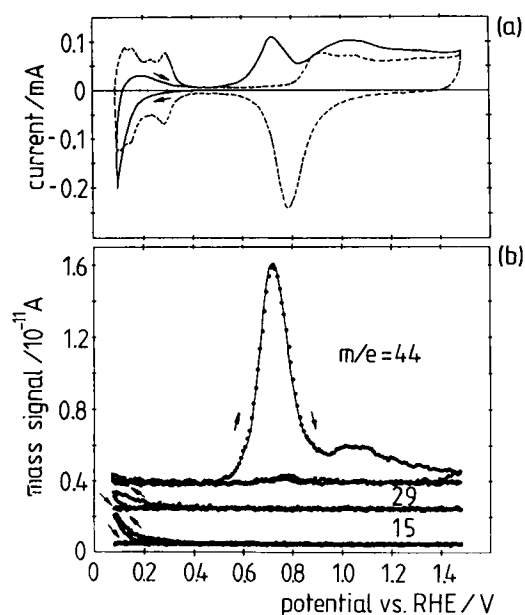


Fig. 5

Oxidation profile of acetaldehyde adsorbate formed out of a 0.05 M  $\text{H}_2\text{SO}_4 + 0.01$  M  $^{12}\text{CH}_3^{12}\text{CHO}$  solution ( $E_{\text{ad}} = 400$  mV,  $t_{\text{ad}} = 200$  s,  $\theta = 0.77$ );  $v = 10$  mV/s; (a) current (—) base electrolyte and (---) adsorbate and (b) mass signal for  $m/e = 15, 29$  and  $44$

For comparison, the desorption properties of acetaldehyde adsorbate were studied in a similar way. Fig. 5 shows the desorption of an  $^{12}\text{CH}_3^{12}\text{CHO}$  adsorbate formed at  $E_{\text{ad}} = 400$  mV during  $t_{\text{ad}} = 200$  s. The final oxidation product  $\text{CO}_2$  ( $m/e = 44$ ) is formed in two clearly separated stages (peak maxima at 720 mV and 1050 mV). Methane ( $m/e = 15$ ) is formed out of the adsorbate as reduction product in

the cathodic scan at potentials lower than 300 mV similar to the case of ethanol adsorbate. But in contrast to the behaviour of ethanol adsorbate the acetaldehyde adsorbate can be reduced again to form acetaldehyde itself. This is evident from mass signal  $m/e = 29$  (main fragment of  $^{12}\text{CH}_3^{12}\text{CHO}$ , intensity 100%) and  $m/e = 43$  ( $\text{M}^+ 1$  signal of  $^{12}\text{CH}_3^{12}\text{CHO}$  with relative intensity ca. 40%, not shown in Fig. 5). Mass signal  $m/e = 44$  shows a slight increase at potentials lower than 300 mV. In this region it represents the unfragmented  $^{12}\text{CH}_3^{12}\text{CHO}$  molecule (relative intensity ca. 60%) with the same potential dependence as masses  $m/e = 29$  and  $43$ . Other mass signals that would reveal reaction products like methanol or ethanol could not be detected.

### 3. In-Situ IR Investigation of Ethanol Oxidation

Base interferograms were recorded using a 15 mm diameter platinum electrode and 1 M  $\text{C}_2\text{H}_5\text{OH} + 0.1$  M  $\text{HClO}_4$  solution at a potential of 50 mV RHE as reference and applying 90 FT scans for averaging. Then the potential was stepped to the working potential for the same number of scans [13, 14].

From the interferograms at reference and working potential the spectra of Fig. 6 are obtained. Spectrum (a) holds for a potential of +400 mV vs. RHE. Only a signal at  $2050$   $\text{cm}^{-1}$  for linearly bonded CO from ethanol adsorption [6, 15] is observed. No reaction product like  $\text{CO}_2$  ( $2341$   $\text{cm}^{-1}$ ) is to be seen.

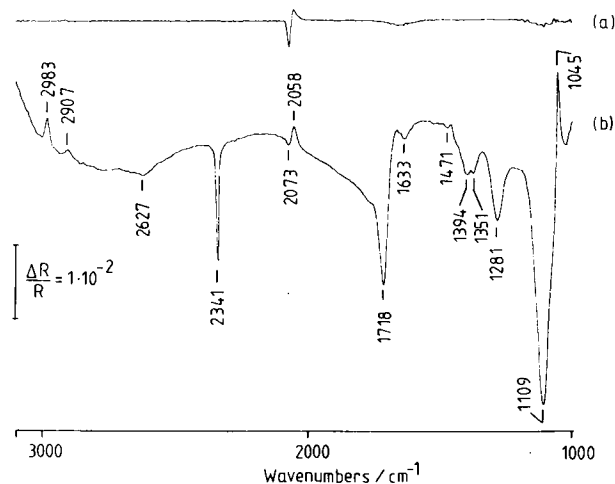


Fig. 6

SNIFTIRS spectra of ethanol on Pt taken in a 0.1 M  $\text{HClO}_4 + 1$  M  $\text{C}_2\text{H}_5\text{OH}$  at 400 mV (a) and 1500 mV (b). Reference spectra at 50 mV

In opposite, using +1500 mV as working potential (spectrum (b) in Fig. 6) several reaction products can be identified [14]:

- $\text{CO}_2$ -formation at  $2341$   $\text{cm}^{-1}$
- acetaldehyde formation (negative going peaks at 1718 and  $1351$   $\text{cm}^{-1}$ )
- acetic acid formation (negative going peaks at 1718, 1394 and  $1281$   $\text{cm}^{-1}$ )
- CO-formation as intermediate of ethanol oxidation (bipolar band at  $2073$  and  $2058$   $\text{cm}^{-1}$ )

- C<sub>2</sub>H<sub>5</sub>OH consumption (positive going peaks at 2983, 2907 and 1045 cm<sup>-1</sup>).

The in-situ IR spectra clearly show that CO is formed as intermediate of ethanol oxidation also at high anodic potential. Beside the final product CO<sub>2</sub> large amounts of acetaldehyde are formed during oxidation.

#### 4. Transfer of the Double Layer to UHV

A detailed study of emersion of the electrode and transfer to UHV must be an integral part of an ex-situ study of electrochemical systems. Two questions are of particular importance:

- Can the particles formed electrochemically be transferred to the UHV chamber intactly or are they decomposed or pumped beforehand?
- Is the sample unacceptably contaminated during the transfer?

The experimental procedure to answer both questions is described in earlier work [6, 7]. The comparison of a flow cell experiment without and with transfer to UHV clearly shows if the chemical composition of the adsorption layer changes during a transfer step. The degree of contamination can be checked by performing a blank experiment.

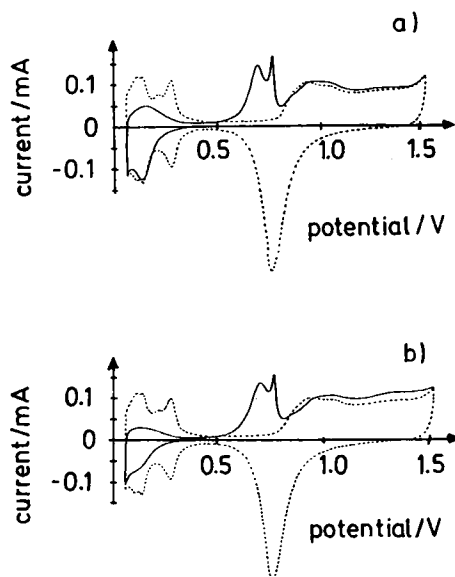


Fig. 7

Oxidation of adsorbed ethanol on Pt ( $R = 1.9$ ) following a flow cell procedure (a), and following a flow cell experiment and transfer to analysis position (b). Adsorption from  $5 \cdot 10^{-3}$  M CH<sub>3</sub>CH<sub>2</sub>OH + 0.1 N H<sub>2</sub>SO<sub>4</sub> at 400 mV RHE for 120 s. (---) Cyclic voltammogram in 0.1 N H<sub>2</sub>SO<sub>4</sub>; 18 mV/s; (—) Cyclic voltammogram in the presence of adsorbed ethanol; 18 mV/s

The voltammogram (a) in Fig. 7 was obtained during oxidation of the adsorbate of ethanol in a flow cell procedure. The  $i$ - $E$  plot (dotted line) was recorded for a Pt sample with a roughness factor  $R$  of 1.9 in 0.1 N H<sub>2</sub>SO<sub>4</sub> with 18 mV/s. Then the potential was stepped from the upper reversal potential of 1.5 V RHE to the adsorption potential of 0.45 V, and the base electrolyte was substituted by 0.1 N H<sub>2</sub>SO<sub>4</sub> +  $5 \cdot 10^{-3}$  N CH<sub>3</sub>CH<sub>2</sub>OH. Adsorption was allowed for 120 s,

then the electrolytic solution was replaced again by 0.1 N H<sub>2</sub>SO<sub>4</sub>. The  $i$ - $E$  plot of the first potential sweep (continuous line) shows the oxidation of the adsorbate; the second sweep proved the bulk ethanol to be quantitatively eliminated during electrolyte exchange.

Voltammogram (b) in Fig. 7 shows the corresponding transfer experiment. The adsorption process was interrupted by exchanging the solutions after 120 s. Then the electrode was emersed and transferred to the surface analysis position in the UHV chamber. After reimmersion a triangular potential scan was applied (continuous line).

The following statements can be derived from a comparison of both experiments:

- Both  $i$ - $E$  plots show an oxidation peak at the end of the double layer region with maxima at  $E_1 = 0.70$  V and  $E_2 = 0.78$  V. The area under these peaks remains unchanged ( $\frac{\Delta Q}{Q} \lesssim 5\%$ ), indicating that the species being oxidized in this potential region survive the transfer to the UHV chamber intact.
- The  $i$ - $E$  plots of both experiments differ considerably in the hydrogen region. An additional cathodic current is observed in the first flow cell experiment. The species involved in this reduction process may be rather weakly bound, so that they are desorbed during the transfer. However, it should be noticed that the amount of charge flowing in the hydrogen region during the cathodic sweep of the transfer experiment still exceeds the amount of charge released in the reversed scan.

In order to prove the validity of the above statement the transfer experiment was performed with different Pt samples using roughness factors  $R$  from 1.3 to 2.7, and in addition using a Pt sample which before had been preferentially orientated to "100" single crystal surface, according to the method of Cervino and Arvia [16]. The result in all cases was as described above. For the following experiments a smooth Pt sheet with a roughness factor of 1.3 was used.

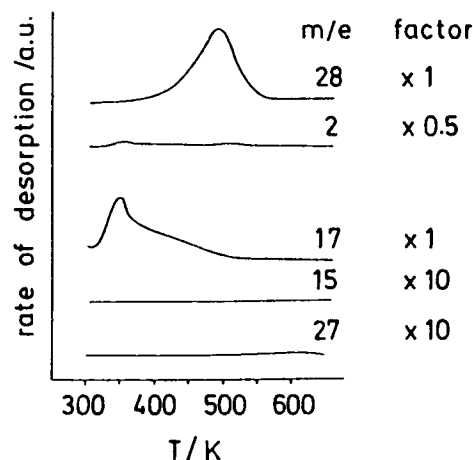


Fig. 8

Blank Experiment. ECTDMS from a Pt electrode after contact with 0.1 N H<sub>2</sub>SO<sub>4</sub> at 400 mV RHE for 120 s. Heating rate  $\beta = 5$  K/s. Desorption spectra for  $m/e = 28$  (CO),  $m/e = 2$  (H<sub>2</sub>),  $m/e = 17$  (OH),  $m/e = 15$  (CH<sub>3</sub>) and  $m/e = 27$  (C<sub>2</sub>H<sub>5</sub>)

### 5. ECTDMS Blank Experiment

Fig. 8 shows the ECTDMS of a Pt electrode which was taken from 0.1 N H<sub>2</sub>SO<sub>4</sub> at 400 mV RHE. For  $m/e = 28$  (CO) a desorption maximum near 500 K was observed. H<sub>2</sub>O yields one peak around 350 K with a shoulder to higher temperatures, as is indicated by the signal for  $m/e = 17$  (OH). The amount of hydrogen ( $m/e = 2$ ) desorbed during the temperature scan is very small, and the signals for  $m/e = 15$  (CH<sub>3</sub>) and  $m/e = 27$  (C<sub>2</sub>H<sub>5</sub>) are virtually zero. The degree of contamination with CO may be expressed via a relative surface coverage  $\theta' = N_{\text{CO}}/N_{\text{CO}}(\text{max})$ .

$N_{\text{CO}}$  and  $N_{\text{CO}}(\text{max})$  are the symbols of CO molecules desorbed during the blank experiment and observed in the desorption spectrum of a Pt electrode at maximum coverage of CO, resp. In the blank experiment of Fig. 8,  $\theta'$  amounts to about 18%; generally it varies between 15% and 20% \*).

### 6. ECTDMS of Ethanol Adsorbate

Fig. 9 shows a series of spectra for  $m/e = 28$  (CO),  $m/e = 2$  (H<sub>2</sub>) and  $m/e = 15$  (CH<sub>3</sub>) recorded during the thermal desorption of ethanol adsorbate on Pt for various initial surface coverages  $\theta'$ . The adsorption layers had been formed electrochemically in a flow cell procedure and the adsorption parameters were chosen as follows:

1	$5 \cdot 10^{-3}$ M CH <sub>3</sub> CH <sub>2</sub> OH + 0.1 N H <sub>2</sub> SO <sub>4</sub> ,	30 s,	400 mV
2	$5 \cdot 10^{-3}$ M CH <sub>3</sub> CH <sub>2</sub> OH + 0.1 N H <sub>2</sub> SO <sub>4</sub> ,	150 s,	400 mV
3	$5 \cdot 10^{-3}$ M CH <sub>3</sub> CH <sub>2</sub> OH + 0.1 N H <sub>2</sub> SO <sub>4</sub> ,	600 s,	400 mV
4	0.1 M CH <sub>3</sub> CH <sub>2</sub> OH + 0.1 N H <sub>2</sub> SO <sub>4</sub> ,	300 s,	400 mV

The desorption diagrams for  $m/e = 28$  (CO) yield one desorption peak around 480 K which slightly shifts to lower temperatures for increasing surface coverage.

A second desorption peak can be observed for high surface coverages [3, 4] as a shoulder in the desorption curves at about 400 K. By analogy with published results for CO desorption from smooth and stepped Pt single crystal surfaces [18], the low temperature peak can be ascribed to the desorption of CO bound to terrace sites, while the high temperature peak is due to CO desorbed from step sites.

The saturation degree of coverage  $\theta'$  amounts to about 0.7 and is obtained for the adsorption parameter of experiment number 3. The spectra for  $m/e = 2$  (H<sub>2</sub>) show desorption maxima near 480 K, which virtually coincide with the second CO peak. Another high temperature desorption state is observed at about 600 K.

The desorption diagrams for  $m/e = 15$  (CH<sub>3</sub>) yield one desorption peak at the temperature of the first CO peak, which increases with increasing adsorption time and ethanol

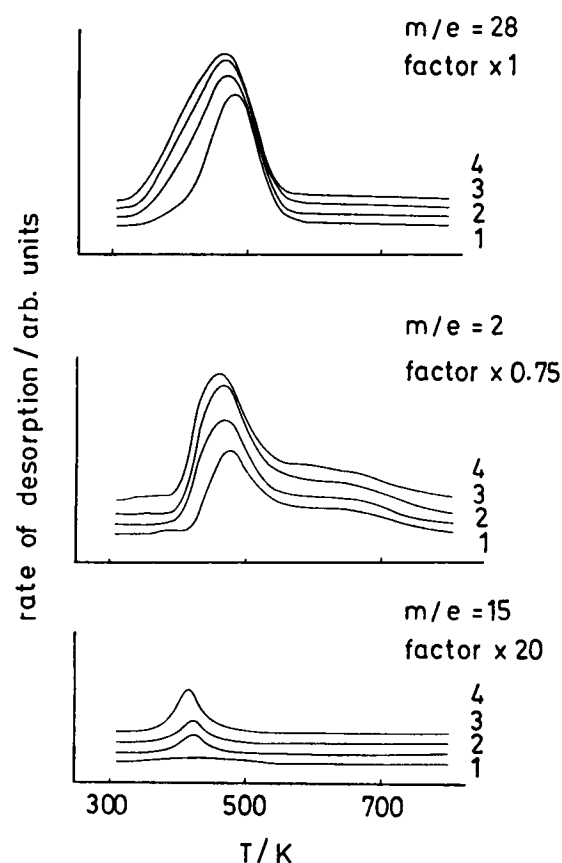


Fig. 9

ECTDMS of ethanol adsorbate on Pt. Heating rate  $\beta = 5$  K/s. The spectra are vertically shifted. Parameter of adsorption were chosen as follows:

- 1 0.1 N H<sub>2</sub>SO<sub>4</sub> +  $5 \cdot 10^{-3}$  N CH<sub>3</sub>CH<sub>2</sub>OH;  $E_{\text{ad}} = 400$  mV RHE;  $t_{\text{ad}} = 30$  s;  $\theta' = 0.46$
- 2 0.1 N H<sub>2</sub>SO<sub>4</sub> +  $5 \cdot 10^{-3}$  N CH<sub>3</sub>CH<sub>2</sub>OH;  $E_{\text{ad}} = 400$  mV RHE;  $t_{\text{ad}} = 150$  s;  $\theta' = 0.56$
- 3 0.1 N H<sub>2</sub>SO<sub>4</sub> +  $5 \cdot 10^{-3}$  N CH<sub>3</sub>CH<sub>2</sub>OH;  $E_{\text{ad}} = 400$  mV RHE;  $t_{\text{ad}} = 600$  s;  $\theta' = 0.64$
- 4 0.1 N H<sub>2</sub>SO<sub>4</sub> + 0.1 N CH<sub>3</sub>CH<sub>2</sub>OH;  $E_{\text{ad}} = 400$  mV RHE;  $t_{\text{ad}} = 300$  s;  $\theta' = 0.63$

Desorption spectra for a)  $m/e = 28$  (CO), b)  $m/e = 2$  (H<sub>2</sub>), c)  $m/e = 15$  (CH<sub>3</sub>)

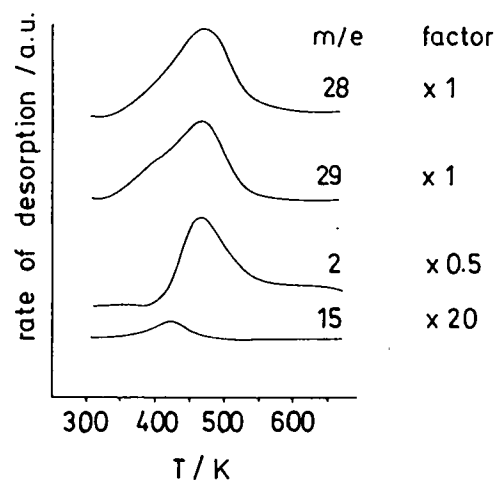


Fig. 10

ECTDMS of ethanol adsorbate on Pt. Adsorption from  $5 \cdot 10^{-3}$  M CH<sub>3</sub><sup>13</sup>CH<sub>2</sub>OH + 0.1 N H<sub>2</sub>SO<sub>4</sub> at 400 mV RHE for 300 s. Heating rate  $\beta = 5$  K/s. Desorption spectra for  $m/e = 28$  (<sup>12</sup>CO),  $m/e = 29$  (<sup>13</sup>CO),  $m/e = 2$  (H<sub>2</sub>),  $m/e = 15$  (<sup>12</sup>CH<sub>3</sub>)

\*) The sticking probability  $s$  of CO is a function of surface coverage. The initial value of  $s$  for Pt(111) is about 0.7 ( $\theta = 0$ ) and drops to  $s \sim 0.35$  for  $\theta = 0.6$  and is about 0.1 for  $\theta = 0.75$  [17]. The effect of the residual gaseous atmosphere observed in the blank experiment is therefore an upper limit. The degree of contamination will decrease drastically in the case of an electrode with an adsorption layer formed electrochemically. This assumption is corroborated by the fact that the difference of charges released during the oxidation of the adsorbates of CO, CH<sub>3</sub>OH and CH<sub>3</sub>CH<sub>2</sub>OH in a flow cell and transfer procedure, is smaller than 5% for sufficient coverages.

concentration; note, however, that these spectra are amplified by a factor of 20 compared with the corresponding desorption diagrams of CO and H<sub>2</sub>. The signals for  $m/e = 31$  (CH<sub>2</sub>OH, fragment of ethanol with highest mass intensity)

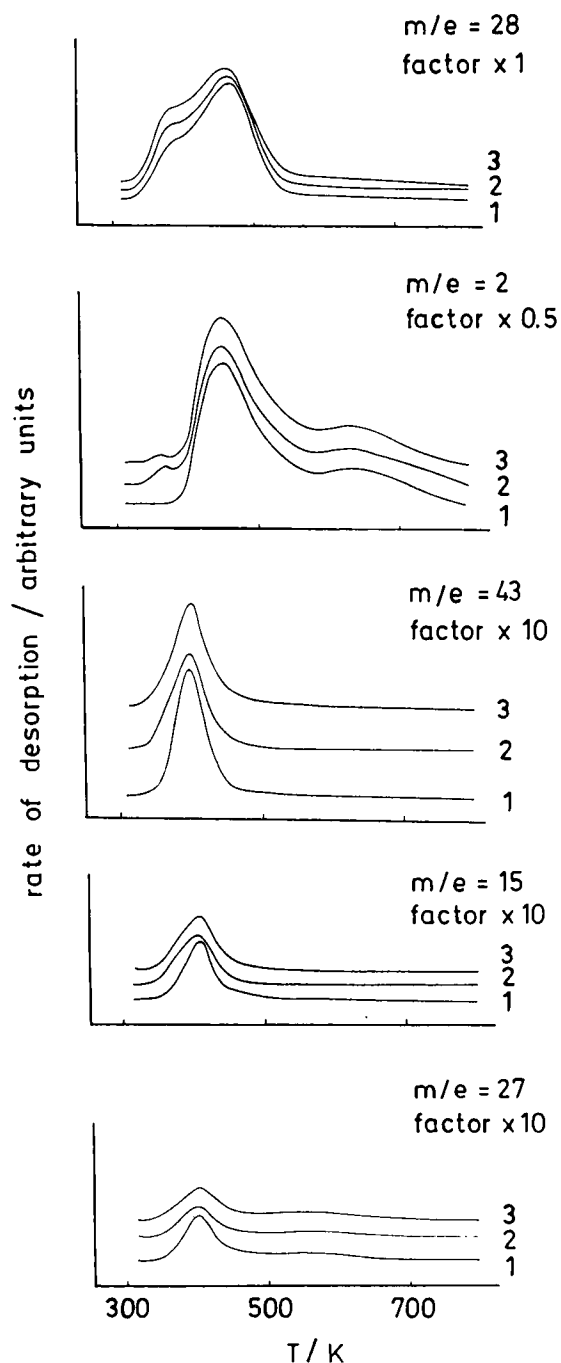


Fig. 11

ECTDMS of acetaldehyde adsorbate on Pt. Heating rate  $\beta = 5$  K/s. Parameter of adsorption and apparent degrees of coverage  $\theta'$ :

- 1  $5 \cdot 10^{-4}$  M CH<sub>3</sub>CHO + 0.1 N H<sub>2</sub>SO<sub>4</sub>, 400 mV RHE, 30 s,  $\theta' = 0.53$
- 2  $5 \cdot 10^{-3}$  M CH<sub>3</sub>CHO + 0.1 N H<sub>2</sub>SO<sub>4</sub>, 400 mV RHE, 30 s,  $\theta' = 0.56$
- 3  $5 \cdot 10^{-3}$  M CH<sub>3</sub>CHO + 0.1 N H<sub>2</sub>SO<sub>4</sub>, 400 mV RHE, 300 s,  $\theta' = 0.62$

Desorption spectra for a)  $m/e = 28$  (CO), b)  $m/e = 2$  (H<sub>2</sub>), c)  $m/e = 43$  (CH<sub>3</sub>CO), d)  $m/e = 15$  (CH<sub>3</sub>), e)  $m/e = 27$  (C<sub>2</sub>H<sub>5</sub>)

and for  $m/e = 43$  (CH<sub>3</sub>CO), not shown in Fig. 9, are virtually zero.

Fig. 10 shows the ECTDMS of the adsorbate of labelled ethanol from Pt after contact with  $5 \cdot 10^{-3}$  M CH<sub>3</sub><sup>13</sup>CH<sub>2</sub>OH + 0.1 N H<sub>2</sub>SO<sub>4</sub> at 450 mV for 300 s. The signals of  $m/e = 29$  (<sup>13</sup>CO) and  $m/e = 28$  (<sup>12</sup>CO) yield peaks around 475 K, which coincide with the low temperature peak of hydrogen ( $m/e = 2$ ). The desorption trace of <sup>13</sup>CO shows a distinct shoulder around 450 K which is only less pronounced in the signal of <sup>12</sup>CO. The ratio of the number of desorbed CO molecules  $N_{^{13}\text{CO}}/N_{^{12}\text{CO}}$  obtained from the integrated thermal desorption spectra amounts to about one. The signal of  $m/e = 15$  (CH<sub>3</sub>) shows a small signal around 450 K.

## 7. ECTDMS of Acetaldehyde Adsorbate

Since acetaldehyde is formed during the bulk oxidation of ethanol (see above), a desorption spectrum of acetaldehyde was taken for comparison (Fig. 11). The adsorption parameters were varied to obtain different surface coverages  $\theta'$ :

- 1  $5 \cdot 10^{-4}$  M CH<sub>3</sub>CHO + 0.1 N H<sub>2</sub>SO<sub>4</sub>, 30 s, 400 mV
- 2  $5 \cdot 10^{-3}$  M CH<sub>3</sub>CHO + 0.1 N H<sub>2</sub>SO<sub>4</sub>, 30 s, 400 mV
- 3  $5 \cdot 10^{-3}$  M CH<sub>3</sub>CHO + 0.1 N H<sub>2</sub>SO<sub>4</sub>, 300 s, 400 mV

Fig. 11a shows the family of desorption traces for CO ( $m/e = 28$ ) at different coverages. The rate of adsorption for acetaldehyde is higher than that for ethanol. A relative degree of coverage  $\theta'$  of 0.53 is obtained with  $5 \cdot 10^{-4}$  M CH<sub>3</sub>CHO at an adsorption time of 30 s and an adsorption potential of 400 mV (1). Two distinct desorption states near 470 K and 380 K are observed for all coverages  $\theta'$ . While ethanol is adsorbed preferentially at step sites, and the population of the terrace sites is low even for high coverages (Fig. 9), the adsorption of acetaldehyde seems to be less sensitive to the morphology of the sample. Adsorption proceeds at terrace sites already for low coverages (1), and the pop-

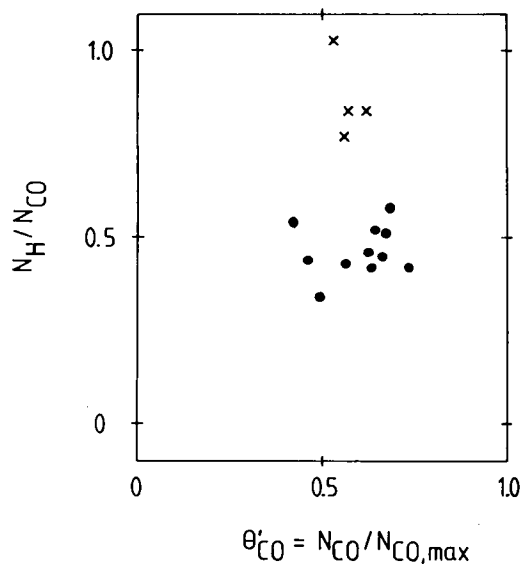


Fig. 12

Ratio of the numbers of desorbed particles  $N_{\text{H}}/N_{\text{CO}}$  from the adsorption layers of ethanol (O) and acetaldehyde (x) on Pt as a function of the apparent degree of coverage  $\theta'_{\text{CO}} = N_{\text{CO}}/N_{\text{CO,max}}$ .  $N_{\text{CO,max}}$  is the number of CO molecules desorbed from a Pt electrode saturated with CO

ulation of the terrace sites is rather high for large coverages. The spectrum of  $m/e = 2$  ( $H_2$ ) (Fig. 11b) yields two desorption peaks at about 470 K and 620 K, the low temperature peak of which coincides with the high temperature peak of CO.

Fig. 11c–e show a series of desorption spectra for  $m/e = 43$  ( $CH_3CO$ ),  $m/e = 15$  ( $CH_3$ ) and  $m/e = 27$  ( $C_2H_5$ ). In all cases desorption peaks are observed coinciding with the low temperature peak of CO.

The number of particles desorbing in the experiment can be evaluated from the area under the desorption curves via calibration measurements. In Fig. 12 the ratio  $N_H/N_{CO}$  is plotted as function of the relative surface coverages  $\theta' = N_{CO}/N_{CO}(\max)$  for ethanol and acetaldehyde adsorbate. This ratio is obviously constant in both cases and amounts to about 0.5 for ethanol and to 0.9 for the acetaldehyde adsorbate.

### Discussion

Our experimental observations lead to the following statements on the mechanism of the anodic oxidation of ethanol on platinum.

1. Ethanol is adsorbed on Pt predominantly dissociatively, and only terrace sites may be populated with adsorbed intermediates with an intact C–C-bond to a minor extent.

Experimental evidence:

- The mass signals for  $m/e = 31$  ( $CH_2OH$ , fragment of  $CH_3CH_2OH$  with the highest mass intensity) and  $m/e = 43$  ( $CH_3CO$ ) do not change during the temperature scan (ECTDMS).
- Since methane does not adsorb on Pt from the gas phase even for a high dosage of 600 L, the adsorption peak for  $m/e = 15$  ( $CH_3$ ) is obviously due to a 2 C surface species. This signal is small and the peak coincides with the low temperature maximum of CO (Fig. 7).
- The desorption of  $CH_4$  observed with on-line MS during the cathodic sweep must be explained by the reduction of a 2 C particle for an analogous reason (even after a prolonged contact (60 min) of the electrode with base electrolyte saturated with  $CH_4$ , the degree of adsorption is virtually zero and no signal for  $m/e = 15$  can be detected during the cathodic sweep). Since no signals for  $m/e = 31$  ( $CH_2OH$ ) and  $m/e = 30$  ( $CH_2O$ , fragment of acetaldehyde) are detected in the cathodic scan, it can be concluded that the 2 C surface species is decomposed during the reduction.

The area under the signal for  $m/e = 15$  ( $CH_3$ ) representing the amount of desorbed  $CH_4$  is small, so that only a minor part of the adsorbed species has an intact C–C-bond.

2. The methyl group and the alcohol group of ethanol is oxidized to COH and CO during the process of adsorption.

Experimental evidence:

- The main desorption products of the adsorbate of ethanol are CO and  $H_2$ , and only small amounts of

$CH_4$  are detected (Fig. 9); the ratio of the adsorbed particles  $N_H/N_{CO}$  is about 0.5 (Fig. 12).

- The desorption spectrum of the adsorbate of ethanol with a labelled hydroxylic C-atom shows desorption traces for both  $m/e = 28$  ( $^{12}CO$ ) and  $m/e = 29$  ( $^{13}CO$ ) (Fig. 10).
- On-line mass spectroscopy shows for the adsorbate of labelled ethanol mass signals for  $m/e = 44$  ( $^{12}CO_2$ ) and  $m/e = 45$  ( $^{13}CO_2$ ) at exactly the same potential of 0.68 V RHE indicating the oxidation of the same surface species (Fig. 4).
- In-situ IRRAS shows CO as ethanol adsorbate and as intermediate of ethanol oxidation.

3. Acetaldehyde is formed as one of the main products during ethanol oxidation (IRRAS and on-line MS), but is not found in detectable amounts in the ethanol adsorbate (on-line MS).

Our findings on the mechanism of ethanol adsorption and oxidation are summarized in Fig. 13.

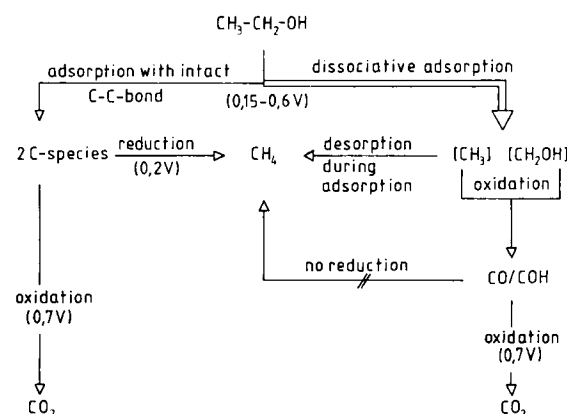


Fig. 13

Schematic diagram for the formation and oxidation of the ethanol adsorbate on platinum in acid solution

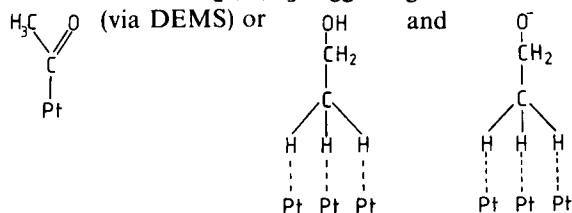
### Conclusions

We have studied adsorption and anodic oxidation of ethanol on platinum applying three independent methods.

Our results clearly show:

- ethanol is adsorbed mainly dissociatively in form of adsorbed CO and COH species (IRRAS and ECTDMS),
- only a minor part of the adsorbate keeps its C–C bond intact, (ECTDMS and on-line MS),
- large amounts of acetaldehyde are formed during ethanol oxidation (on-line MS and IRRAS),
- the ethanol adsorbate is formed directly out of bulk ethanol and not via acetaldehyde,
- in the hydrogen region during cathodic scan methane can be detected as desorbed products in the presence of ethanol adsorbate and/or bulk ethanol (on-line MS),
- with large amounts of acetaldehyde in solution the reformation of this species in the hydrogen region is observed (on-line MS).

Earlier statements [2, 4, 5] suggesting C—C adsorbates like



(via IRRAS) could not be confirmed.

This work was supported by the European Communities under contract EN 3-E0072D, by Siemens AG and by the Deutsche Forschungsgemeinschaft (DFG).

We are indebted to Dr. T. Iwasita for leaving us the FTIR spectra and to P. Königshoven for solving technical problems.

### References

- [1] A. Kutschker and W. Vielstich, *Electrochim. Acta* **8**, 985 (1963).
- [2] J. Willsau and J. Heitbaum, *J. Electroanal. Chem.* **194**, 27 (1985).
- [3] K. D. Snell and A. G. Keenan, *Electrochim. Acta* **194**, 1683 (1982).
- [4] J. Willsau and J. Heitbaum, *Electrochim. Acta* **31**, 943 (1986).
- [5] B. Beden, M. C. Morin, F. Hahn, and C. Lamy, *J. Electroanal. Chem.* **229**, 353 (1987).
- [6] S. Wilhelm, W. Vielstich, H. W. Buschmann, and T. Iwasita, *J. Electroanal. Chem.* **229**, 377 (1987).
- [7] S. Wilhelm, T. Iwasita, and W. Vielstich, *J. Electroanal. Chem.* **238**, 383 (1987).
- [8] T. Iwasita, W. Vielstich, and E. Santos, *J. Electroanal. Chem.* **229**, 367 (1987).
- [9] O. Wolter, C. Giordano, J. Heitbaum, and W. Vielstich, *Proc. Symp. Electrocatalysis*, p. 235, The Electrochem. Soc., Pennington 1982.
- [10] E. Cattaneo, B. Bittins-Cattaneo, W. Vielstich, and P. Königshoven, *Analyt. Chem.*, in preparation.
- [11] S. Wilhelm, thesis University of Bonn 1988.
- [12] A. Bewick and S. Pons, in: "Advances in Infrared and Raman Spectroscopy", Vol. 12, p. 1, R. J. H. Clark and R. E. Hester (Eds.), Wiley Heyden (1985).
- [13] P. A. Christensen and A. Hamnet, in: "Comprehensive Chemical Kinetics", C. H. Bamford and R. G. Compton (Eds.), in preparation.
- [14] T. Iwasita, B. Rasch, E. Cattaneo, and W. Vielstich, *Electrochim. Acta*, in press.
- [15] H. Seki, K. Kunitatsu, and W. Golden, *Appl. Spectra* **39**, 437 (1985).
- [16] R. M. Cervino, A. J. Arvia, and W. Vielstich, *Surf. Sci.* **154**, 623 (1985).
- [17] R. A. Shigeishi and D. A. King, *Surf. Sci.* **58**, 379 (1976).
- [18] D. M. Collins and W. E. Spicer, *Surf. Sci.* **69**, 85 (1977).

Presented at the 87th Annual Meeting of the Deutsche Bunsen-Gesellschaft für Physikalische Chemie "Neue Entwicklungen in der Elektrochemie" in Passau, from May 12th to May 14th, 1988

## Measurement of Mass and Surface Stress at One Electrode of a Quartz Oscillator

K. E. Heusler, A. Grzegorzewski, L. Jäckel, and J. Pietrucha

Abteilung Korrosion und Korrosionsschutz, Institut für Metallkunde und Metallphysik, Technische Universität Clausthal, D-3392 Clausthal-Zellerfeld

### Adsorption / Electrochemistry / Methods and Systems / Surface Stress

The theory for the calculation of changes of mass and surface stress from frequency measurements at a quartz oscillator subject to different on-sided pressures is outlined. The various contributions to apparent changes of the mass are discussed. Experiments refer to the determination of effective molar masses of potassium ions and fluoride ions during electrostatic adsorption and of chemisorbed lead both on polycrystalline gold by a comparison of masses to charges. Effective molar masses of adsorbed species can also be determined by comparison of mass changes to surface concentrations e.g. determined by the radiotracer method as in the example of the adsorption of chloride at the passivating oxide film on iron. The density of very thin films like the passivating oxide film can be obtained by comparing mass changes to thicknesses from optical measurements. In agreement with theoretical expectation, compressive surface stresses were qualitatively found for the underpotential deposition of lead on gold. In the growing oxide film on passive iron very large compressive lateral pressures were observed.

### Introduction

Sauerbrey [1] demonstrated that changes of the resonance frequency of a quartz oscillator are proportional to mass changes of the electrodes on one or both sides of the quartz disc. The quartz oscillator is a very sensitive balance. It was used for investigations of the reaction kinetics between solids and gases [2, 3] and, more recently, of electrochemical reactions between solid electrodes and an electrolyte [4–8]. A theory was developed to calculate effective molar masses of species transferred in ion transfer reactions [4]. From electrochemical measurements at a quartz fre-

quency balance with the electrode in the electrolyte being a rotating disc electrode, the effective molar masses of manganese ions and oxygen ions transferred at manganese dioxide in acid manganese sulfate solutions were calculated.

The resonance frequency of a quartz oscillator was observed to depend also on the elastic energy stored in the quartz disc [9, 10]. This effect provides the possibility to measure simultaneously changes of mass and surface stress at one of the two electrodes of the quartz oscillator. After an outline of the theory, first experimental results are presented.